Anodic film growth on Ru/Pt electrodes in HClO$_4$ and HCl solutions

F. COLOM

Instituto de Química Física CSIC. Serrano 119, 28006 Madrid, Spain

M. J. GONZÁLEZ-TEJERA

Departamento de Química Física, Facultad Ciencias Químicas, Universidad Complutense, 28040 Madrid, Spain

The voltammetric formation and potentiostatic growth of anodic films on Ru/Pt electrodes in HClO$_4$ and HCl solutions were studied by single negative potential sweeps and cathodic charging curves in the potential range from −0.25 to 1.1 V vs SCE. The growth of the anodic layer proceeds through the formation of two layers of different reduction reversibility. At potentials below 500 mV, the layer more reversibly reduced, grows slowly to a maximum coverage equivalent to one oxygen monolayer. The thicker, and more stable, layer increases with holding time to a maximum of about three oxygen monolayers during the period of time studied (7 h). At holding potentials above 500 mV, the reduction charge of the anodic layer reaches a constant value after polarization for 1 h. Growth starts with formation of two layers which, with time, become a single layer which is hardly reducible. The results suggest the eventual formation of anhydrous RuO$_2$. In HCl solutions, Cl$^-$ adsorption inhibits the formation of the anodic layer, decreasing its growth rate but reaching no limiting thickness for 7 h. At holding potentials below 650 mV vs SCE, only a single layer is formed with slight structural changes. At potentials above 650 mV, the initially homogeneous film converts with holding time into a bilayer where the outer layer becomes hardly reducible. This layer is assumed to be a stable anionic hydroxy species (RuCl$_5$OH^{2-}) which dissolves as Ru$_2$O$_2$Cl$_6$(H$_2$O)$^{2-}$. In HClO$_4$ and HCl the layer growth follows a direct logarithmic law.

1. Introduction

Oxide formation and corrosion on ruthenium electrodes is of great interest in the chloralkali industry due to the successful application of dimensionally stable anodes (DSA) with thermally prepared RuO$_2$ on a titanium substrate [1].

The formation and growth of thick oxides on ruthenium electrodes has been studied by Rand *et al.* [2] and Conway and coworkers [3–5] by repetitive potential cycling in H$_2$SO$_4$ solution. The latter authors [4] found that, at short times and under potentiostatic conditions, the oxide film grows following a direct logarithmic law. The same anodic growth law was found for Ru/Pt electrodes in sulphuric acid solutions at high concentration (12 M) when polarized at constant potential above 0.75 V vs RHE [6]. In this case, after the potentiostatic polarization, a negative sweep gave a cathodic peak whose potential shifted linearly to more negative values with logarithm of time.

Wider information on the electroformation of oxide films on electrodeposited ruthenium electrodes in HClO$_4$ and HCl solutions, both by a single potential sweep and at constant positive potential, is reported here. The anodic films were studied by negative potential sweeps and cathodic galvanostatic charging curves.

2. Experimental details

Ruthenium electrodes were prepared by electroplating the metal on platinum foils (Ru/Pt) from Ru(NO)Cl$_3$ (ICN Pharmaceuticals Inc) solutions as described elsewhere [7]. A platinum-mesh counter-electrode of large area and a thermostated two-compartment cell were used. Electrolytes were prepared with Riedel de Haën HClO$_4$ and HCl analytical grade reagents with triply distilled water. The reference electrode was a saturated calomel electrode (SCE), which was connected to the cell through a double electrolyte bridge of HClO$_4$ solution. Potentials are referred to the SCE unless otherwise stated. Nitrogen was used for deoxygenation.

Potentiodynamic curves were obtained with a Wenking POS 73 Potentioscan connected to a Hewlet–Packard 3466 digital millivoltmeter and registered in a Sefram BG recorder. The slow cathodic potential-time transients were recorded on a Sefram Servorac B.P. instrument. An ultrarapid mercury relay LTE 394 (R) was used to switch the potentiostat to galvanostatic conditions.

Prior to the potentiostatic measurements the working electrode was polarized at or near −250 mV vs SCE for 15 min. Because of the difficulty in measuring the real area of the electrode, current density

and charge densities are referred to the apparent surface of the electrode.

3. Results

3.1. *In 1 M HClO$_4$*

The potentiodynamic behaviour of a freshly electrodeposited Ru electrode (Ru/Pt) in HClO$_4$ solutions exhibits marked activity in the potential range of oxide formation. Cyclic voltammograms of this electrode from the hydrogen (-250 mV vs SCE) to the oxygen evolution region (about 1, 2 V) show an anodic peak at around 750 mV and one or two cathodic peaks, depending on the positive limit of the potential sweep (Fig. 1), as described in a previous paper [8].

The negative sweeps, recorded after holding the anodic potential scan at a given value, E_p, for different times, show an increase in the reduction charge with time. The voltammograms from the hydrogen evolution region to positive potentials lower than 400 mV vs SCE show a broad cathodic peak which increases with time with no shift of the peak potential. The cathodic current increases markedly with time in the hydrogen region as can be seen for $E_p = 175$ mV vs SCE in Fig. 2.

Potential cycling to 400 mV shows a cathodic shoulder that becomes a peak if the potential is held at 400 mV, along with a slight shift of the peak potential (Fig. 3). At potential sweep limits above 400 mV, two cathodic peaks are recorded which move to more negative potentials with time and, eventually, overlap in the hydrogen evolution region, as shown in Fig. 4 for the potential limit at 750 mV.

The potentiostatic growth with time of the ruthenium oxide film in HClO$_4$ follows a direct logarithmic law as illustrated in Fig. 5, where the total reduction charge increases linearly with log t, with larger slopes at higher potentials. The reduction charge reaches a constant value after 1 h polarization at potentials above 500 mV. At lower potentials no limit is detected in the film growth up to 7 h. As
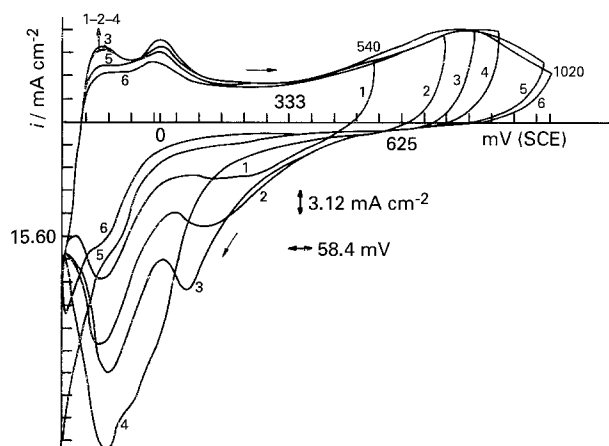

Fig. 2. Negative voltammetric curves of oxide grown potentiostatically at 175 mV vs SCE during several polarization times: (a) 30 s, (b) 300 s, (c) 3600 s and (d) 25 000 s. Electrodes in 1 M HClO$_4$; cycled at 10 mV s^{-1}.

shown in the inset, the growth rate ($dQ/d\log t$) increases linearly with the holding potential. Thus, these results coincide with those for Ru electrodes in H$_2$SO$_4$ [4, 6] at short times (up to 1000 s) but otherwise disclose a limiting oxide thickness in HClO$_4$. No such limit has been observed in 1 M HCl (Fig. 6) for periods from 30 s to 7 h.

These results are consistent with the known increase in hysteresis with time in the formation and reduction of surface oxides in other platinum group metals. The cause of this hysteresis has been ascribed to different processes, for instance, different formation and reduction rates of the anodic film, or a controlling diffusion process in the reduction reaction, or structural changes in the anodic film due to a place exchange process between metal and oxygen atoms.

The results given in Figs 1 and 4 point to the reduction process of the oxide film formed by anodic sweeps up to high positive potentials being similar to that of

Fig. 1. Cyclic voltammetry at Ru/Pt electrodes in 1 M HClO$_4$ solutions from -250 mV vs SCE to increasing anodic limit potentials at 10 mV s^{-1}.
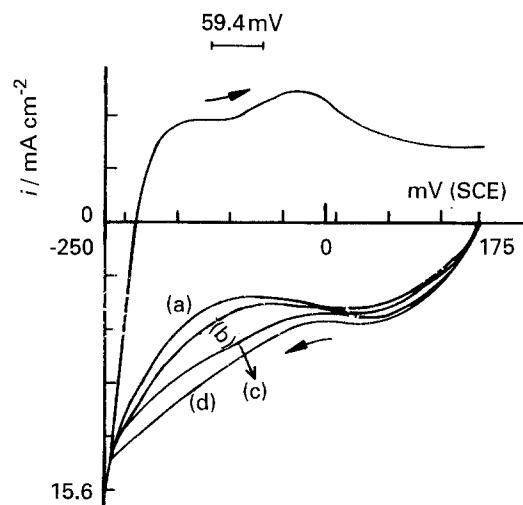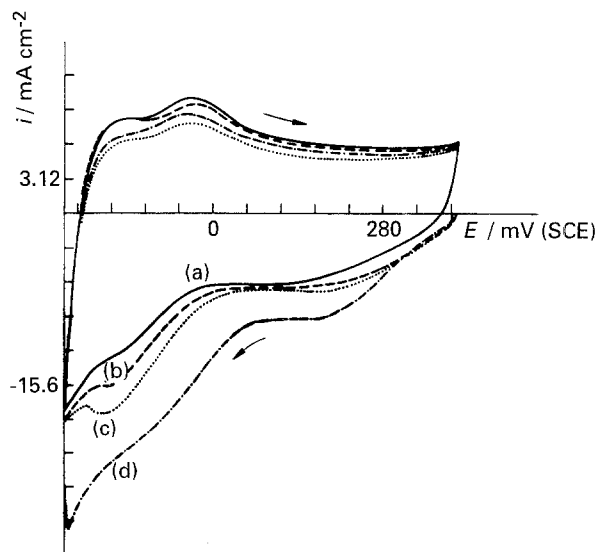

Fig. 3. Voltammetric reduction of ruthenium oxides grown at 400 mV for different periods of time: (a) 0 s, (b) 60 s, (c) 300 s and (d) 21 600 s. Electrodes in 1 M HClO$_4$; cycled at 10 mV s^{-1}.
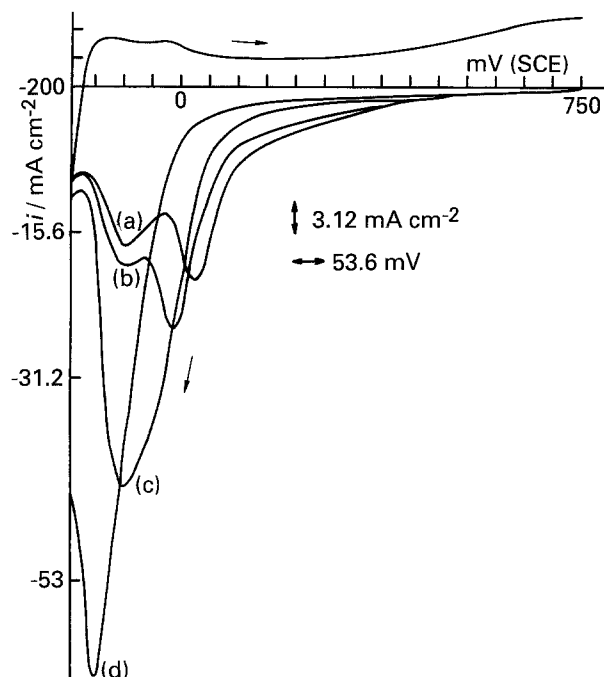
Fig. 4. Cathodic voltammetry of Ru/Pt electrodes potentiostatted at 750 mV vs SCE in 1 M HClO₄ for different times: (a) 30 s; (b) 60 s; (c) 300 s; (d) 11 100 s. Cycling at 10 mV s⁻¹.

the film formed potentiostatically between 400 mV and the oxygen evolution region. Two energy states of oxygen bonded to the metal can be distinguished: one of which is more reversibly reduced over a wide potential region, which may be ascribed to chemisorbed oxygen, and another which may correspond to hydrous oxide or hydroxide, and is reduced at more negative potentials. At high potentials, or long potentiostatic polarizations, both types of oxygen compounds become a single, hardly reducible film oxide. It can be assumed that at quite low potentials (about −40 mV vs SCE), oxidation of water molecules provides a growing layer of adsorbed oxygen. This
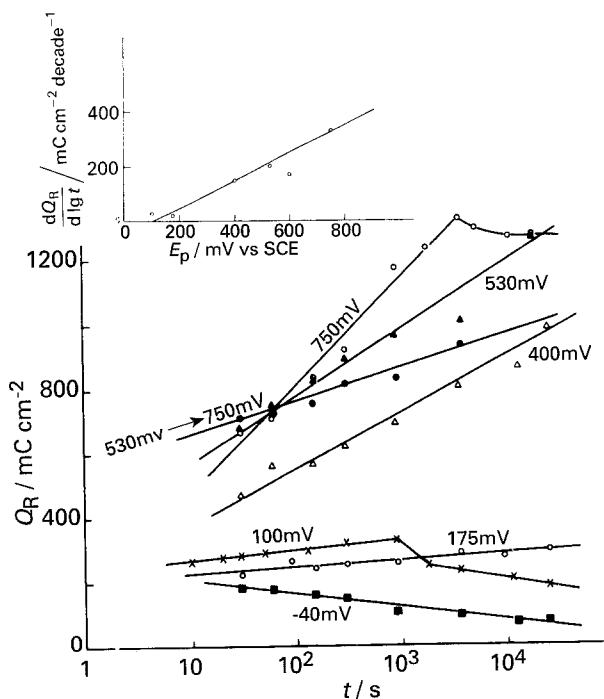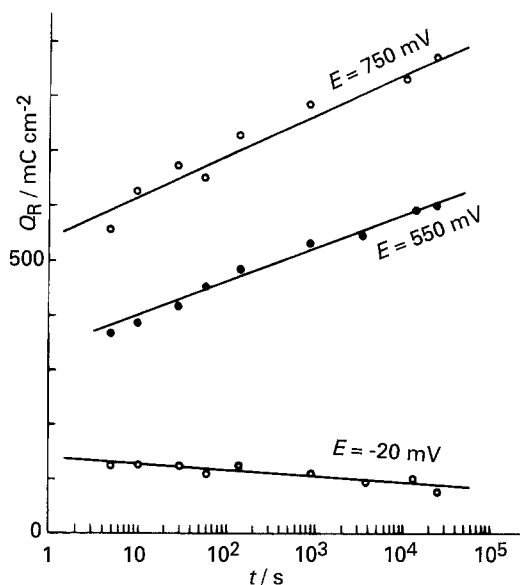

Fig. 6. Increase of the reduction charge with time obtained by potential sweeps at 10 mV s⁻¹ after potentiostatic polarization of Ru/Pt in 1 M HCl at different potentials. Cycling at 10 mV s⁻¹.

oxygen, under the effect of the electric field and through a place exchange mechanism, changes into a more thermodynamically stable layer oxide. Figures 1 and 4 suggest that for anodic sweeps to potential limits above 700 mV vs SCE the adsorbed oxygen becomes a more stable oxygen compound, so that two different oxides coexist. At higher potentials or long polarizations these two oxides become a single homogeneous layer, probably an increasingly dehydrated RuO_2 with an electrochemical behaviour similar to that of thermally prepared RuO_2/TiO_2 [1].

To check the lability of the anodic film formed at a given potential and its influence on the further oxidation of the film, the positive sweep was held at this potential for different times, after which, the potential cycle was completed. In Fig. 7 a voltammetric sweep from −250 to 750 mV vs SCE, with potential
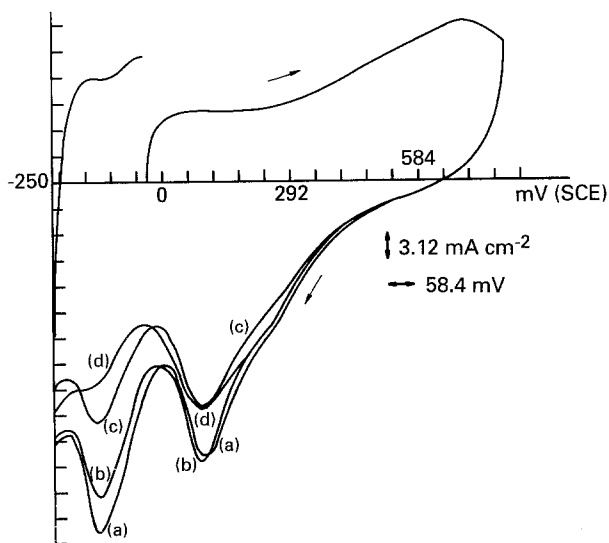

Fig. 5. Growth of the reduction charge with log t of the ruthenium oxide formed at different constant potentials. Inset: variation of $dQ_r/d \log t$ with potential.

Fig. 7. Cyclic voltammetry at Ru/Pt electrodes in HClO₄ from −250 to 750 mV vs SCE after holding the potential scan at −40 mV for different times: (a) 30 s, (b) 300 s, (c) 3600 s and (d) 25 200 s. Cycling at 10 mV s⁻¹.
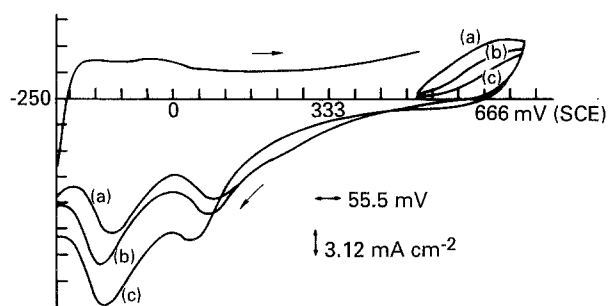
Fig. 8. Cyclic voltammetry at Ru/Pt electrodes in $HClO_4$ from -250 to $750\,mV$ vs SCE after holding the potential sweep at $530\,mV$ at $10\,mV\,s^{-1}$ for several times: (a) $30\,s$, (b) $300\,s$ and (c) $3600\,s$.

holding at $-40\,mV$ for different times, is given. No marked change in the negative sweeps was observed for short holding times. In contrast, for times longer than $900\,s$ the cathodic peak currents decrease with time. This implies that at $-40\,mV$ vs SCE (in the hydrogen region) the ad- or absorbed hydrogen increases with time and reacts with the adsorbed OH or incipient oxide, so preventing the thickening of the oxygen layer. For potentials held about $530\,mV$ (Fig. 8), the following oxidation to $750\,mV$ shows the increasing passivation of the electrode with time. Nevertheless, the negative curves are similar to those for coverages grown at $750\,mV$, (Figs 4 and 8). As shown in Fig. 5, the total cathodic charge for the film reduction increases in a linear way with log t but the growth rate is lower than that for $530\,mV$, in spite of the further oxidation to $740\,mV$. This implies that the growth of the oxide layer at $530\,mV$ does not essentially affect the constitution of the Ru oxide

formed at higher potentials, but inhibits its further oxidation as reported also for Pt [9].

The nature of these two types of oxygen bond to the Ru metal (adsorbed oxygen and oxide) is confirmed by the cathodic charging curves obtained at Ru/Pt electrodes after anodic voltammetric sweeps. As illustrated in Fig. 9, the charging curves at layers grown at $750\,mV$ vs SCE for $30-300\,s$ show two potential arrests, which coincide with the two cathodic current peaks in Fig. 4 and correspond to thermodynamically stable layers. At longer polarization times, the charging curves show a rapid desorption of oxygen, followed by a long potential arrest which becomes more negative with time. That is, the oxygen coverage grows more homogeneous and irreducible with time.

On electrodes polarized at 530 and $400\,mV$ vs SCE, a pseudocapacity at high potentials, followed by a potential arrest at more negative values is recorded. The growth of the total oxygen layer is linear with log t, reaching a limiting reduction charge at shorter times the higher the potential over $500\,mV$. At lower polarization potentials no growth limit is observed. The separate plot of the oxide reduction and oxygen desorption charge reveals the increase of the total oxygen layer to be mainly due to oxide formation as the oxygen adsorption increases slightly with time (Fig. 10). These results are thus consistent with those obtained by voltammetric techniques.

The cathodic charging curves on ruthenium electrodes in $1\,M$ $HClO_4$ at -75, -50 and $10\,mV$ vs SCE show the capacitive charge of the double layer followed by hydrogen discharge and eventual evolution at $-270\,mV$. Hydrogen discharge otherwise exhibits
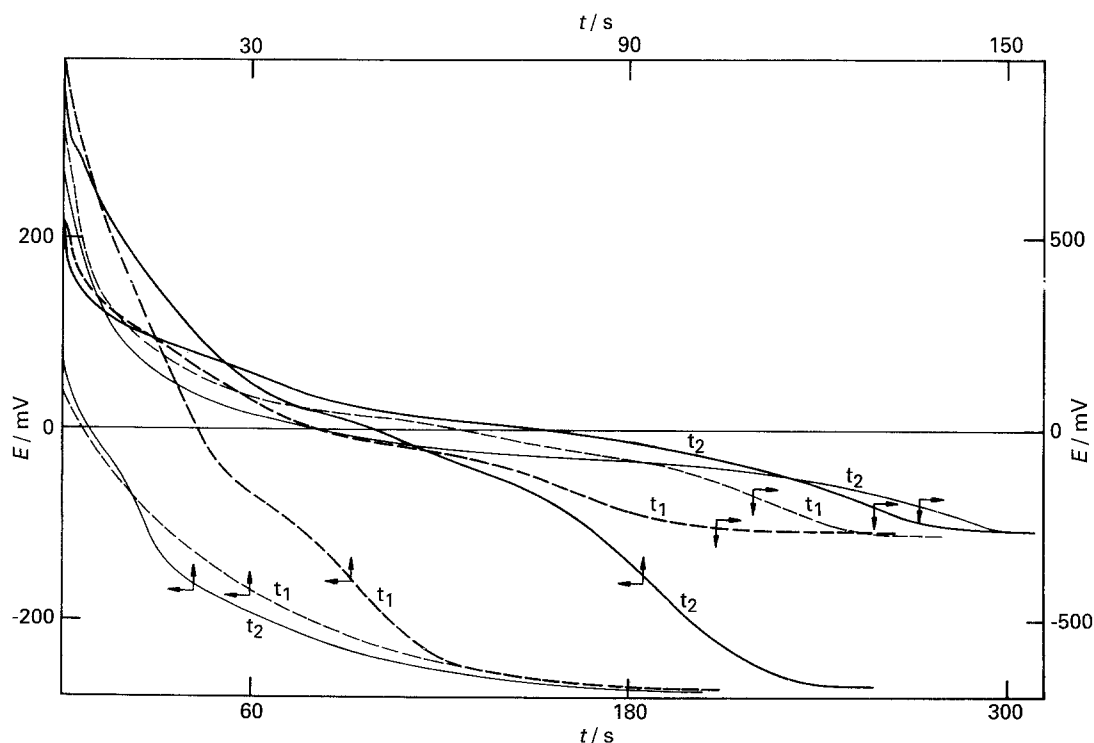

Fig. 9. Cathodic charging curves at constant current density, $3.12\,mA\,cm^{-2}$, at ruthenium electrodes, potentiostatted at different anodic potentials for diverse periods of time. In $1\,M$ $HClO_4$, $V_1 = 100\,mV$, $V_2 = 400\,mV$ and $V_3 = 530\,mV$, $t_1 = 30\,s$, $t_2 = 25\,200\,s$; $V_4 = 750\,mV$, $t_1 = 60\,s$, $t_2 = 25\,200\,s$.
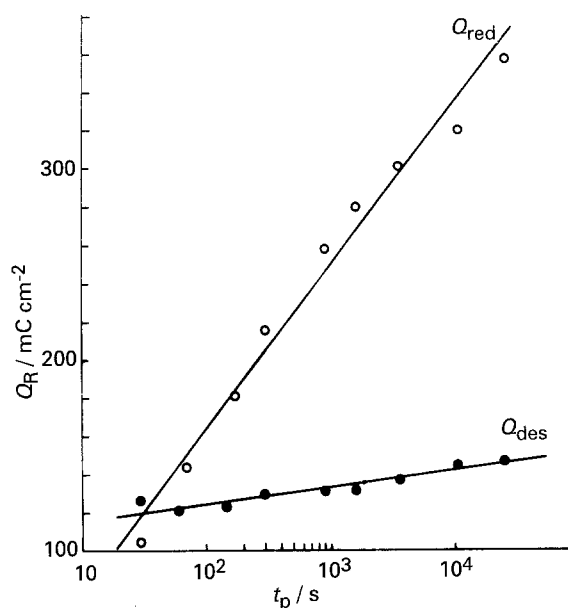
Fig. 10. Growth of oxygen desorption (pseudo capacity) and oxide reduction charge with time at Ru/Pt electrodes at 400 mV vs SCE calculated by cathodic charging curves. 1 M $HClO_4$, $i = 3.12$ mA cm^{-2}, $E_p = 400$ mV.

a rising overpotential with longer polarization, i.e. from -100 to -190 mV in the period from 300 to 25 200 s, which is ascribed to the inhibiting effect of ruthenium oxidation on that process. Oxygen adsorption at this potential range was shown through cyclic voltammetry by Conway et al. [3, 4] who pointed out the reversible adsorption of oxygen and growth of the oxygen layer at -50 mV vs SCE in 0.5 M H_2SO_4 at 20 °C and almost reversible stages of surface oxidation at -50 to 150 mV vs SCE overlapping with adsorbed and desorbed H-oxidation [4].

In the charging curves for anodic film formed at potentials above 100 mV vs SCE a pseudocapacity is observed from about -100 to -230 mV vs SCE that seems to correspond to adsorption of hydrogen, although it could include some oxygen reduction. This hydrogen adsorption charge remains constant, or increases slightly, with polarization time; this may be taken as a tentative estimation of a monolayer of adsorbed hydrogen, hence oxygen coverage or oxide thickness. Thus, from films grown at 400 mV vs SCE, the oxygen to ruthenium atom ratio results in Ru_2O_3 (this compound is not thermodynamically stable [10] so the formation of $Ru(OH)_3 \cdot H_2O$ [11] or RuOOH [12] must be assumed). The thermodynamic data for ruthenium hydroxide gives E^0(Ru/ $Ru(OH)_3H_2O) = 0.65$ V [11] which would account for the experimental results. At 530 mV vs SCE, the oxygen coverage amounts to formation of RuO_2 after polarization for 1 h, which coincides with the Pourbaix [10] E^0 (Ru_2O_3 hyd/RuO_2 hyd) $= 0.937$ V, and the experimental value E^0 ($Ru(OH)_3H_2O/$ RuO_22H_2O) between 0.90 and 0.95 V [11].

At 750 mV vs SCE, two different oxygen layers make up a mixed hydroxide/oxide compound ($Ru(OH)_3$ and RuO_2) with the eventual formation of RuO_2 according to the chronopotentiograms.

3.2. In 1 M HCl

To check the influence of the anion on the formation of the anodic film, cyclic potentiodynamic curves were recorded at Ru/Pt electrodes in 1 M HCl solutions. The negative potential sweeps (Fig. 11) show a similar structure to those obtained in $HClO_4$, except for the higher anodic potential required to obtain the cathodic current peak shifts in HCl. However, a more homogeneous and hardly reducible layer is formed in $HClO_4$ at high oxidation potentials, with only one eventual reduction peak, than in HCl solutions where two types of surface oxi-compounds are detected, even at potentials of Cl_2 evolution. Thus the overall reduction process is more reversible in HCl than in $HClO_4$, which implies that Cl^- adsorption inhibits the deep oxidation of the electrode and prevents the formation of a homogeneous and irreducible surface oxide at high potentials. On the other hand, the hydrogen discharge overpotential is higher at the anodic films formed in $HClO_4$ than in HCl.

At sweep limits above 1100 mV vs SCE corrosion and dissolution of the electrode gives rise to a yellow solution whose spectrophotometric analysis, immediately after the potential sweep, yields absorption peaks at 255, 272, 350–60 nm and 450 nm. The spectra correspond to the binuclear Ru(IV) compound $Ru_2O_2Cl_6(H_2O)_2^{2-}$ according to [13].

This anion must be formed by anodic dissolution of some Ru-oxy-chloride compound from the electrode surface since no rapid reaction of ruthenium oxides with HCl is known under the experimental conditions. One of these possible compounds is the well known binuclear $Ru_2OCl_{10}^{4-}$ [13] which is very stable in solid state and acid solutions but in 1 M HCl rapidly decomposes into $Ru_2OCl_8(H_2O)_2^{2-}$ [14] and finally in $Ru_2O_2Cl_6(H_2O)_2^{2-}$ [15].
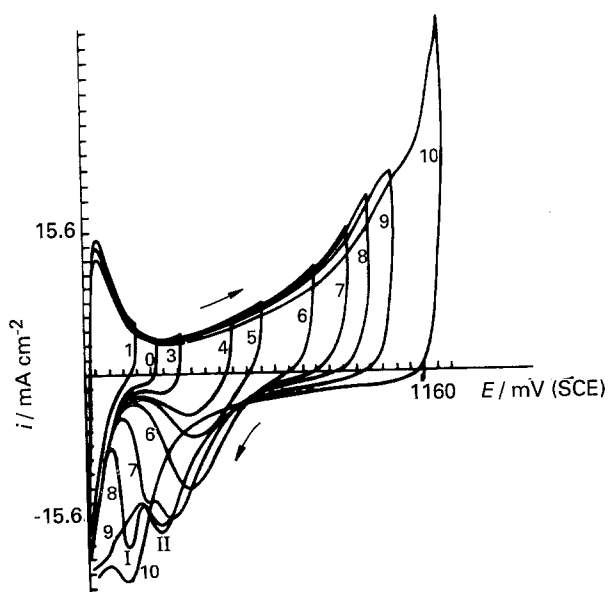

Fig. 11. Voltammetric cycles recorded at Ru/Pt electrodes in 1 M HCl from -270 mV to increasing anodic potentials at 10 mV s^{-1}. Cycling at 10 mV s^{-1}.

This suggestion is supported by the potential-pH diagram published by Loucka [16] for the Ru–H_2O–Cl system at 25°C which predicts the formation of $RuCl_5(OH)^{2-}$ under these experimental conditions. This anion is experimentally found only in the binuclear form $Ru_2OCl_{10}^{4-}$ [13].

Some singular features are detected for anodic layer growth at constant potential in 1 M HCl (Fig. 6). The negative potential sweeps from -20 mV vs SCE show a reduction wave whose current density decreases with time followed by a rapid increase at more cathodic potentials due to hydrogen discharge and evolution. The decrease in oxygen adsorption at -20 mV given in Fig. 6 coincides with the increase in Cl⁻ adsorption on ruthenium with time which is maximum at about 200 mV vs RHE as proved by Horanyi and Rizmayer by the radiotracer method [17]. The cathodic voltammograms for oxides grown at 550 mV show only one single oxygen desorption peak in contrast to the two peaks observed in HClO₄ (Fig. 12). The peak poten-

tial is more positive in HCl than in HClO₄ and shifts slightly to cathodic potentials with time. That is, the anodic layer on ruthenium in HCl turns out more homogeneous and reversibly reduced than in HClO₄ at the same potential. The layer increases in thickness but largely maintains its structure.

At potentials higher than 750 mV, ageing of the homogeneous layer after 30 s of polarization produces two cathodic current peaks in the negative potential sweep. The more cathodic peak moves with time to the hydrogen region more rapidly than the less cathodic one (Fig. 12). These results suggest that, in this potential range, the constant adsorption of oxygen builds up a layer that is restructured with time, forming a second surface compound much more stable and similar to that formed by potential sweeps to high potentials (Fig. 11).

Comparison of anodic coverage and growth rate at Ru/Pt electrodes in HCl and HClO₄ proves both values to be lower in HCl. This confirms the competitive influence of Cl⁻ ion adsorption on the anodic oxidation of ruthenium.

4. Discussion

As is known, potential sweep techniques can produce structural and reproducible voltammograms at ruthenium electrodes only if slow potential scans are applied [2–8]. However, overlapping at low potentials between currents due to hydrogen and oxygen (or OH) deposition or removal makes it very difficult to assess the true surface area of the electrode and hence oxide thickness. The nature and composition of the anodic film on ruthenium electrodes has been the subject of several studies with different techniques and discrepant results [18]. Thus, the anodic film has been regarded as a thick phase oxide of composition ranging from RuO to RuO_2 or as a few oxygen monolayers built up by the successive adsorption and discharge of H_2O molecules. Nevertheless, repetitive potential cycling of the electrode from 0.05 V vs RHE to values over 0.8 V has been proved to produce a thick, reversible surface oxide, similar to that observed on iridium, with porous structure and columnar morphology [3–5, 19].

The results reported in the present work support the hypothesis of thin layer formation through the gradual buildup of a few oxygen monolayers with eventual composition of anhydrous RuO_2.

The anodic current peak registered around 750 mV vs SCE in Fig. 1 is usually attributed to hydrated RuO_2 formation [2–8] $E^0(Ru_2O_3$ hyd/RuO_2 hyd) = 0.937 V [10]. At potentials above 1.1 V a rise in electric current is observed with oxygen evolution and dissolution of the electrode as RuO_4.

The high anodic current recorded in the voltammograms points to strong oxidation processes although no significant feature is registered before RuO_2 formation. This may be due to the instability of ruthenium oxide or hydroxide with oxidation states lower than 4, specially in the presence of oxygen. Thermody-
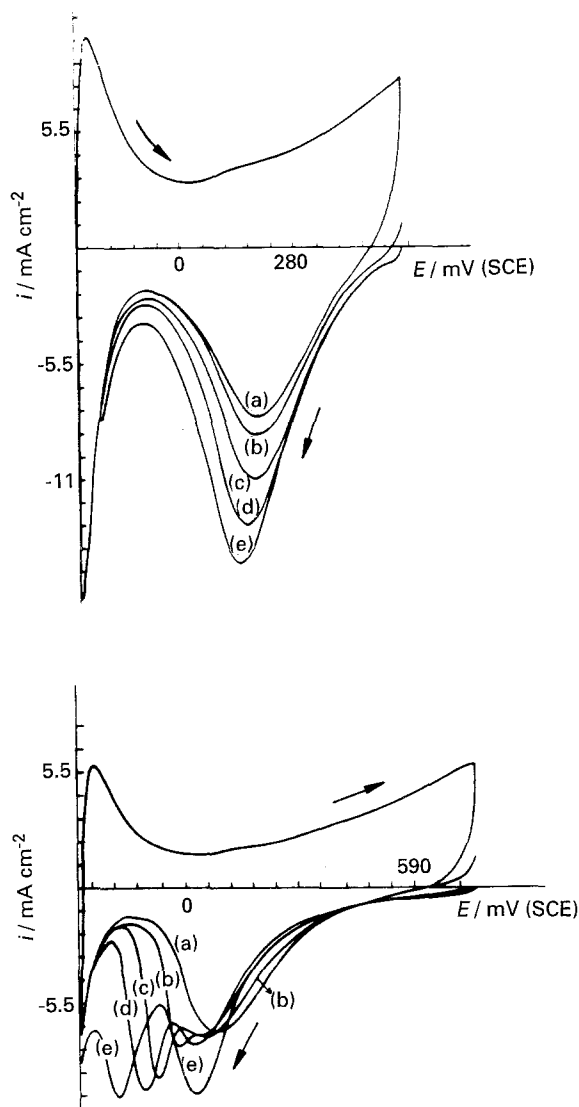

Fig. 12. Cathodic voltammetry of Ru/Pt electrodes in 1 M HCl after holding the potential at 550 mV vs SCE (upper) for different times: (a) 0 s, (b) 30 s, (c) 150 s, (d) 3600 s and (e) 25 200 s. Similarly for lower curves at 750 mV vs SCE for (a) 0 s, (b) 30 s, (c) 150 s, (d) 900 s and (e) 25 200 s. Cycling at 10 mV s⁻¹.

namic data indicate that Ru(III) hydroxide and RuO_2H_2O are metastable so that the hydroxide can disproportionate to Ru, RuO_2 and H_2O, and the oxide dehydrate spontaneously [11]. This agrees with the fact that RuO_2 is the only oxygen compound clearly identified in work on anodic films on Ru. Moreover, new thermodynamic data for RuO_2 formation, $E^0(Ru/RuO_2) = 0.57$ V [1, 12] may account for the stable phase, probably hydrous RuO_2, produced at 400 mV vs SCE (Fig. 10).

Ellipsometric studies [20] and XPS analysis [21] of the oxygen film formed on ruthenium in H_2SO_4 solution suggest the adsorption of a monolayer of oxygen and OH in the potential range up to 1.1 V vs SCE which becomes an oxide at higher potential and hydrated RuO_2 about 1.5 V. The SNIFTIRS spectra for ruthenium in $HClO_4$ [22] show no i.r. bands for OH adsorption or any change in oxidation state of he metal up to 1.3 V vs RHE. This is consistent with the i.r. transparency found for RuO_2 and its rapid formation by disproportionation of Ru(III) compounds.

The large electric charges involved in the formation and growth of the anodic oxide on ruthenium here reported may be, in part, related to the large roughness factor. In fact, about 500 was estimated for Ru/ Pt in $HClO_4$ [8], in agreement with that calculated by Bagotzkii et al. [23]. Also, the same value is deduced from hydrogen adsorption in the cathodic charging curves (Fig. 9) if a monolayer of hydrogen is assumed to be 0.28 mC cm^{-2} of real area for ruthenium according to [23]. In this case, the anodic film in 1 M $HClO_4$ amounts to a limiting value of about four monolayers of oxygen at 750 mV vs SCE. Even allowing for a large error of the roughness factor the results are near to the growth of a thin film of the type reported in [18].

The direct logarithmic law (Figs 5 and 10) can be written as

$$Q_r = \Delta Q \log t + B \qquad (1)$$

where Q_r is the film reduction charge; $\Delta Q = dQ_r/d \log t$ depends linearly on the potential (Fig. 5) and B, the charge at 1 s, is a function of E.

The growth rate is then

$$i_a = \frac{dQ}{dt} = \left(\frac{dQ}{d \log t}\right)\left(\frac{1}{2.3t}\right)$$

$$= \frac{\Delta Q}{2.3t} = i_{t=1}\left(\frac{1}{t}\right) \qquad (2)$$

That is, the current for film formation decreases with time, as experimentally observed, and is proportional to the slope ΔQ of the log plot.

From Fig. 5, the slope ΔQ can be written as

$$\Delta Q = C\eta \qquad (3)$$

where η is measured from the potential E where the slope is zero, i.e. with no growth or negligible increase with time of the anodic film, and C is a parameter.

Thus from Equation 1,

$$Q_r = C\eta\frac{\ln t}{2.3} + Q_{r(t=1)}$$

hence

$$t = \exp\left[\frac{2.3(Q_r - Q_{r(t=1)})}{C\eta}\right] \qquad (4)$$

which with Equation 3 in Equation 2 yields

$$i_a = \frac{C\eta}{2.3}\exp\left[\frac{-2.3(Q_r - Q_{r(t=1)})}{C\eta}\right]$$

This equation, as shown by Gilroy for platinum [24], corresponds to the growth law of a process controlled by the nucleation rate for the case of cylindrical nuclei [25], and therefore to that determining the anodic film formation on ruthenium. Indirect evidence on the ruthenium oxidation state at potentials where RuO_2 is assumed to be formed is given by the dissolution of the metal in HCl around 1.1 V vs SCE reported above, where Ru(IV) chemical species and no compound with higher oxidation state for ruthenium have been found.

The above results may be compared to those for hydrous oxide formation on noble metals [9, 18, 26–29]. The two types of reduction process (Figs 1–4, 9 and 10) are related to the reduction of the inner compact oxygen–metal layer and the outer, relatively thicker oxide layer, with higher water content, discussed in the cited references.

The reduction of films formed at potentials below 700 mV vs SCE shows a capacitative electric charge (Fig. 9) equivalent to less than an oxygen monolayer (Fig. 10), that is, to electrodesorption of an oxygen or HO$^-$ inner layer in the potential range 0.45–0.05 V vs SCE. Reduction starts always at about 450 mV vs SCE where RuO_2 is thermodynamically unstable [11], but where Ru(III) oxy-compounds remain stable

$$E^0\left(\frac{Ru}{Ru(OH)_3H_2O}\right) = 0.65 \text{ V},$$

$$E^0\left(\frac{Ru}{Ru_2O_3hyd}\right) = 0.738 \text{ V}$$

and points to the process

$$Ru(IV) + e^- = Ru(III)$$
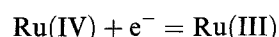
The inner layer becomes more homogeneous and stable when the anodic sweep exceeds 550 mV as revealed by the sharpening and shift of the reduction peak to less positive potentials. The reduction of the outer layer, thicker than the inner one (Fig. 10), proceeds through a current peak in the hydrogen region (from 40 to −240 mV) fitting the reduction of a homogeneous, stable phase. As in the case of gold and platinum [9, 26–29] overlapping of the reduction currents indicate an inhibition effect of the inner layer reduction on that of the thicker outer layer.

Last, the influence of the solution pH on the electrochemical behaviour of the thick oxide layer was not studied, so the formation of this as a stable anionic

hydroxy species, as proposed by Burke et al. [18, 28] for noble metals, cannot be substantiated. However, this could be the case for ruthenium in HCl solutions at 750 mV vs SCE (Fig. 12), where the reduction sweep produces two cathodic current peaks after ageing of the initial homogeneous layer. The fast shift with time of the more cathodic peak potential to more negative values coincides with the formation of $RuCl_5OH^{2-}$ (in the binuclear form $Ru_2OCl_{10}^{4-}$) on the electrode, which goes rapidly into solution as $Ru_2O_2Cl_6(H_2O)_2^{2-}$. This would mean that the increasing irreducibility of the outer layer would correspond to formation of stable anionic hydroxy species.

Nevertheless it must be stressed that a careful study of the formation and reduction of the anodic layer on ruthenium by in situ optical techniques is necessary in order to clear out the nature of such a layer and confirm some of the results discussed in the bibliography.

5. Conclusions

The potentiostatic growth of the anodic film on Ru/Pt electrodes in HClO$_4$ formed by a voltammetric run in the potential range from 0 to 1.1 V vs SCE proceeds through the formation of two layers of different reduction reversibility at potentials below 500 mV vs SCE. Both layers grow following a direct logarithmic law. The inner layer increases slowly with holding time and never exceeds an oxygen monolayer coverage. The outer layer grows more rapidly up to three oxygen monolayers during the time studied (7 h).

At holding potentials above 500 mV vs SCE the reduction charge of the anodic layer becomes constant after one hour. Growth starts with formation of two layers which, after some time, become a single one, homogeneous and hardly reducible. The results suggest that the eventual formation of one or two layers of RuO$_2$ inhibits the further growth of the anodic film.

In HCl solutions, the oxygen coverage is lower than in HClO$_4$ due to the inhibiting effect of Cl$^-$ adsorption. The layer growth also follows a direct logarithmic law but the anodic film does not reach a limiting thickness in the time studied (7 h). At potentials lower than 650 mV vs SCE, the anodic film increases with formation of one single layer, which becomes more stable with time.

At potentials above 650 mV vs SCE, where hydrated RuO$_2$ can form, the initial homogeneous anodic layer divides with holding time into two layers. The inner layer, presumably hydrated RuO$_2$, increases with time and becomes slightly more stable. The outer layer becomes more rapidly irreducible, probably by converting into the anionic hydroxy species RuCl$_5$OH^{2-} (this exists experimentally only in

the binuclear form Ru$_2$OCl$_{10}^{4-}$), and dissolves into solution as Ru$_2$O$_2$Cl$_6$(H$_2$O)$_2^{2-}$.

References

[1] S. Trasatti and W.E. O'Grady, in 'Advances in Electrochemistry and Electrochemical Engineering', vol. 12, (edited by H. Gerischer and Ch. W. Tobias), (1981) p. 177.
[2] R. Woods, D. A. J. Rand and D. Michell, J. Electroanal. Chem. 89 (1978) 11.
[3] S. Hadzi-Jordanov, H. Anderstein-Kozlowska, M. Vukovic and B. E. Conway, J. Phys. Chem. 81 (1977) 2271.
[4] S. Hadzi-Jordanov, H. Angerstein-Kozlowska, M. Vukovic and B. E. Conway, J. Electrochem. Soc. 125 (1978) 1471.
[5] B. E. Conway, H. Angerstein-Kozlowska and M. Vukovic. J. Appl. Electrochem. 12 (1982) 193.
[6] R. O. Lezna, N. R. de Tacconi and A. J. Arvia, J. Electroanal. Chem. 151 (1983) 193.
[7] F. Colom and M. J. González-Tejera, J. Electroanal. Chem. 190 (1985) 243.
[8] F. Colom and M. J. González-Tejera, An. Quim. 85 (1989) 177.
[9] A. C. Chialvo, W. E. Triaca and A. J. Arvía, J. Electroanal. Chem. 146 (1983) 93; 171 (1984) 303.
[10] M. Pourbaix, 'Atlas d'Equilibres Electrochimiques' Gauthier-Villars, Paris (1963) p. 343.
[11] J. A. Rard, Chem. Rev. 85 (1985) 1.
[12] G. Barral, J. P. Diard and G. Montella, Electrochim. Acta 31 (1986) 277.
[13] E. A. Seddon and K. R. Seddon, 'The Chemistry of Ruthenium', Oxford/New York, Elsevier (1984) p. 91–175.
[14] J. P. Deloume, G. Duc and G. Thomas-David, Bull. Soc. Chim. France (1981) 129.
[15] Y. G. Tikhonov, V. A. Bodnya and V. P. Alimarin, Vestn. Mosk. Univ. Khim. 16 (1975) 714.
[16] T. Loucka, J. Appl. Electrochem. 20 (1990) 522.
[17] G. Horanyi and E. M. Rizmayer, J. Electroanal. Chem. 181 (1984) 199.
[18] L. D. Burke and M. G. E. Lyons, 'Modern Aspects of Electrochemistry', Vol. 18, (edited by R. E. White, J. O'M Bockris and R. E. Conway), Plenum Press. London (1986) p. 227.
[19] V. Birss, R. Myers, H. Angerstein-Kozlowska and B. E. Conway, J. Electrochem. Soc. 131 (1981) 1502.
[20] L. N. Velikodnii, V. A. Shepelin, G. J. Zagradzkaya and E. V. Kasatkin, Electrokhimiya 17 (1981) 1397 and 18 (1982) 1275.
[21] R. Kötz, H. J. Lewerenz and S. Stucki, J. Electrochem. Soc. 130 (1983) 825.
[22] A. Bewick, G. Larramona, and C. Gutierrez, J. Electroanal. Chem. 332 (1992) 155.
[23] V. S. Bagotzkii, A. M. Skundin and E. K. Tuseeva, Elektrokhimiya 8 (1972) 1341 and 9 (1973) 54; Electrochim. Acta 21 (1976) 29.
[24] D. Gilroy, J. Electroanal. Chem. 71 (1976) 257.
[25] M. Fleischmann and H. R. Thirsk, in 'Advances in Electrochemistry', Vol. 3 (edited by P. Delahay), Interscience, New York (1963) p. 123.
[26] M. E. Vela, R. C. Salvarezza and A. J. Arvia, Electrochim. Acta 35 (1990) 117.
[27] L. D. Burke and M. MacRann, J. Electroanal. Chem. 125 (1981) 387.
[28] L. D. Burke, J. F. Healy, K. J. O'Dwyer and W. A. O'Leary, J. Electrochem. Soc. 136 (1989) 1015.
[29] L. D. Burke and J. F. O'Sullivan, J. Electroanal. Chem. 285 (1990) 195.